A Practical Distance Measurement Improvement Technique for a SFCW-based Health Monitoring Radar

Marco Mercuri[1], Ping Jack Soh[1,2], Dominique Schreurs[1], and Paul Leroux[3,4]

[1]KU Leuven, Div. ESAT-TELEMIC, Leuven, Belgium
[2]Universiti Malaysia Perlis, School of Computer & Communication Engineering, Perlis, Malaysia
[3]Thomas More Kempen, Div. IBW-RELIC, Geel, Belgium
[4]KU Leuven, Div. ESAT-MICAS, Leuven, Belgium

***Abstract* — A technique in improving the distance measurement of an indoor Stepped-Frequency Continuous Wave (SFCW) radar is proposed and presented in this work. The main objective of this SFCW radar is to enable a non-invasive way in measuring the location of patients in a home environment without the need for a worn geo-locating tag. The theoretical and practical operation principle of the radar setup is first explained. Due to its operation in an indoor environment using a two-antenna setup, reflections, multipath, backscattering and cross-coupling are expected to affect its localization estimation. Thus a compensation technique based on Inverse Fast Fourier Transform (IFFT) is used to overcome this limitation. Practical measurements conducted in a 5 x 5 m^2 room have successfully proven that the approach is able to compensate for practical multipath from walls, furniture and metallic shelves, yielding a distinct improved measurement technique in localizing a person in a real indoor environment.**

***Index Terms* — Calibration, distance measurement, patient monitoring, radar measurements, remote monitoring, SFCW radar, tag-less localization.**

I. Introduction

Non-invasive indoor localization of a human subject by means of radar techniques is typically challenging due to the effects of multipath and reflections existent in a practical indoor environment [1]. Moreover, the ultra-wideband (UWB) nature of the radar architecture combined with the real room setting poses design challenges. In particular, the crosstalk between transmit and receive antennas is a challenge when attempting to arrive at a compact system size combined with a semispherical antenna radiation pattern to cover a full room. Another important challenge is the backscattering, as the radar sensor is to be fixed on the wall or ceiling.

To our knowledge, investigations dealing with these practical issues do not exist. In [2], multiple SFCW radars are used in a through-the-wall localization application. However, the use of bulky and widely spaced horn antennas resulted in negligible crosstalk and backscattering. Moreover, a bulky vector analyzer is used for signal generation, measurement of the radar returns, and to calibrate any delay through cables that connect the ports to the antennas. In [3], a Frequency Modulated Continuous Wave (FMCW) radar is presented for indoor localization. However, large and directive antennas are used to limit multi-path, backscattering and crosstalk. Moreover, a radio frequency identification (RFID) tag is involved to increase the target reflectivity. In [4], a combination of a CW radar and a gyro sensor attached to the target is used for indoor localization. In [5], a complex carrier-based UWB architecture is presented for localization. It involves picoseconds pulses, noncoherent receivers, modelling of complex propagation channels with severe multipath effects, and the need for extremely high sampling rates for digital processing. Moreover, testing is performed by tracking a robot.

In this work, a technique for Stepped-Frequency Continuous Wave (SFCW) radars in measuring a target's distance in a real room environment is proposed and discussed. Compared to [2]-[5], it features a simple, low-cost, and compact distance measurement approach, avoiding the need for both a high-speed data acquisition and related bulky and complex hardware, besides being focused on solving practical issues. Although the proposed approach has been tested using an SFCW radar, the proposed solutions in overcoming practical issues in a practical room setting can be also adopted by other ultra-wideband systems.

In this paper, the radar architecture and the operation principle are first presented. Next, the technique to measure the target's absolute distance is discussed. Finally, results of the measurements before and after the technique's implementation are shown in the experimental results.

II. Radar Working Principle

A SFCW waveform is generated by the radar, sent towards a human target, and its echo is collected and processed by the receiver. The resulting baseband signals are then digitized and sent through a serial port to a laptop to determine the target's absolute distance.

Fig. 1 shows the experimental radar set-up. It consists of a Fractional-N Phase-locked Loop (PLL) with a wideband Voltage-controlled Oscillator (VCO), a wideband power divider, a low noise amplifier (LNA), a gain block, an In-phase and Quadrature (IQ) mixer, baseband circuitry, and a microcontroller. The latter programs the synthesizer of the PLL to generate the SFCW waveform and it also acquires the

I and Q baseband components to be transmitted serially to a laptop. The system has been built using off-the-shelf components, except for the antennas which have been custom designed. The main antenna design challenge was to minimize crosstalk as well as backscattering, while maintaining a semispherical radiation pattern. The crosstalk is due to the radar's compactness (antennas cannot be spaced out far apart), whereas the backscattering is due to the radar's mounting on the wall or ceiling. These two undesired effects have as consequence that the total receiver's gain has to be decreased as to avoid the saturation of both the amplifiers and ADC. As a result, the reflection of a weak target becomes no longer perceptible by the ADC's resolution. This situation occurs when a person is located far away from the radar. The resulting custom designed antennas based on the coplanar waveguide (CPW) bow-tie topology [6] are shown in Fig. 2. This custom design has been verified to be operational, as shown in Fig. 3. The use of a common ground plane strongly reduces the backscattering, while the metal wall suppresses the crosstalk between the two elements (S_{21}), maintaining a satisfactory reflection coefficient (S_{11}).

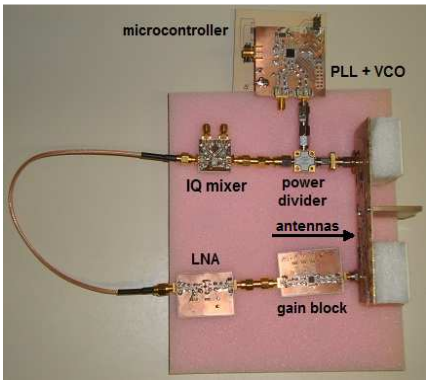

Fig. 1. Experimental SFCW radar set-up. Picture of the RF part, microcontroller, and antennas.

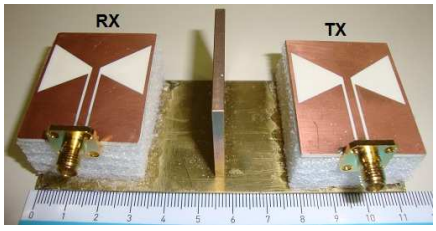

Fig. 2. Two-element bow-tie antenna prototype.

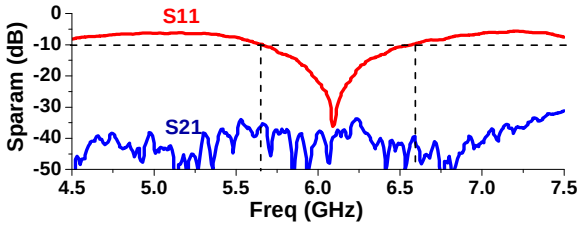

Fig. 3. Measured antenna S-parameters.

The SFCW radar transmits a waveform that consists of N = 21 coherent CW pulses (called *burst*) whose frequencies are increased pulse by pulse by a fixed increment of Δf = 25 MHz. Each pulse is about T = 105 µs long, resulting in a burst duration of about $N{\cdot}T$ = 2.2 ms. Its total bandwidth, $N{\cdot}\Delta f$ = 525 MHz operates between 6 and 6.525 GHz enabling a smallest distance resolution of about 28.57 cm.

Neglecting the initial amplitudes, the SFCW waveform can be expressed as:

$$T_{SFCW}(t) = \cos\left[2\pi\left(f_0 + n\Delta f\right)t + \varphi_n(t)\right] \qquad (1)$$

for $0 < t \le N{\cdot}T$, with $0 \le n < N$. If the waveform is reflected by a target at a distance D, the received signal will then be represented as:

$$R_{SFCW}(t) = \cos\left[2\pi\left(f_0 + n\Delta f\right)\left(t - \frac{2D}{c}\right) + \varphi_n\left(t - \frac{2D}{c}\right)\right]. \qquad (2)$$

The output of the IQ mixer can be modeled as the product of the received signal with a copy of the transmitted signal followed by a lowpass filter. For a quadrature sampling, it is given as:

$$e^{-j\phi_n} = I(t) + jQ(t) \qquad (3)$$

with

$$\phi_n = 2\pi\left(f_0 + n\Delta f\right)\frac{2D_n}{c} + \theta_n + \Delta\varphi_n(t) \qquad (4)$$

where

$$\Delta\varphi(t) = \varphi(t) - \varphi\left(t - \frac{2D}{c}\right) \qquad (5)$$

is the negligible residual phase noise, while θ is the contribution of the ca. 180° phase shift reflected at the target surface, plus the additional phase difference between the mixer and the antenna. Only one sample for pulse width T has been considered. In the case of a moving target, the range D can be written as:

$$D_n = D_0 + v(t_n)nT \qquad (6)$$

where D_0 is the range to the target at the particular time $t = 0$. Combining eq. (6) with eq. (4), the phase of the baseband signal becomes:

$$\phi_n = \frac{4\pi f_0 R_0}{c} + 2\pi\frac{\Delta f}{T}\frac{2R_0}{c}nT + 2\pi\frac{2v(t_n)f_0}{c}nT + 2\pi\frac{2v(t_n)n\Delta f}{c}nT + \theta_n \qquad (7)$$

Equation (7) is used to determine the target's absolute distance. The first two terms represent a stationary target since they are not influenced by speed, $v(t)$. The first term represents a constant phase shift, which is practically insignificant, while the second term represents the multiplication between the rate of frequency change Δf / T and the signal round-trip time

$2D / c$. This frequency shift can then be converted into the target range profile by performing an Inverse Fast Fourier Transformer (IFFT) of the received signal from N frequency-stepped CW pulses. The third term represents the Doppler frequency shift due to target motion, which adds to the frequency shift of the second term, resulting in a shift of target distance from its true value. The fourth term exists due to the interaction of the frequency-varying step waveform with the target's motion, resulting in a signal spread of the target peak. Compensating these effects is difficult due to the unknown instantaneous target velocity. However, they can be neglected by properly choosing the burst duration $N{\cdot}T$ such that the target is considered static during this interval, namely considering that the speed $v(t)$ is equal to 0. The burst interval of 2.2 ms is sufficiently short to consider this condition to be true. Moreover, this ensures also that the downconverted signals of the SFCW waveform consist of I/Q direct current (DC) levels (Fig. 4). This means that only two samples have to be acquired per pulse width T. The final term is frequency-dependent and adds a fixed frequency shift to the actual target distance. For the proposed radar, this is approximately 85 cm. This term is compensated using a calibration procedure during data processing. It should be noted that a fixed increment Δf of 25 MHz enables a 6 m coverage, of which about 5.15 m can be used for the desired target range and the remaining 85 cm is to accommodate for the fixed shift.

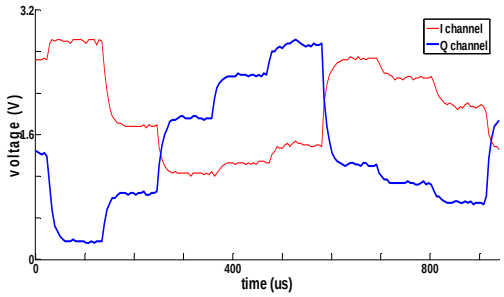

Fig. 4. Measured I and Q baseband signals of the stepped frequency waveform. The pulse width T is about 105µs. Each pulse reaches its DC level after a settling time. After that time, the signal is acquired.

III. Distance Estimation Technique

The digitized I/Q baseband signals are processed using Matlab. They are first related as in eq. (3) and then the target's range profile is determined applying the IFFT to the N complex samples. However, the main measurement challenge is to distinguish the target's reflection from the effects of backscattering and crosstalk. The latter involve strong reflections that overwhelm the much weaker reflected/received signal, resulting in the inability to acquire any meaningful target information. Moreover, the reflections produced by furniture present in practical environments must also be tackled. Both factors have been eliminated by a compensation procedure that consists in determining an environmental range profile, characterizing the total contribution from crosstalk, backscattering and cluttering. Its magnitude is then subtracted from the range profiles obtained with the target in the room. Next, the range profile is shifted by 85 cm to compensate for the effect of the fifth term in eq. (7). This value is obtained through calibration placing a flat metal plate at a known distance from the antennas. The value of its corresponding peak in the range profile is subtracted to its calibrated distance yielding θ_n. However, it has to be mentioned that this operation can be only successful if the backscattering and crosstalk have been strongly reduced at first.

IV. Experimental Results

Experimental measurements have been conducted with two human volunteers of similar 1.75 m height and different weights, located at different radial distances in the room. The radar has been fixed to the wall at 1.5 m of height. Furniture and metallic shelves are deliberately included to enable the existence of clutter and reflections, mimicking a typical room setting. The results of the data processing routine can be seen in Fig. 5. Fig. 5a represents an initial range profile of a person at 3 m away from the antennas, prior to the compensation and calibration process. The peak, indicating the target's absolute distance, is totally buried in the undesired reflections. In particular, the crosstalk represents the most dominant effect as indicated by the strong peak at about 85 cm. This also indicates the position of the two antennas in the range profile, which ideally should be at 0 m. As expected, it results shifted in the range by the contribution of the fixed frequency shift θ_n. Applying the compensation and the calibration steps, the target's peak can be properly resolved as shown in Fig. 5b. It should be noted that although the person was at 3 m away the antennas, he resulted located at about 2.86 m in the range profile. This happens because the radar has a range resolution of about 28.57 cm. For that reason, any target's physical distance will be rounded to the nearest location/resolution provided by the radar. This also establishes the maximum error in localization of about 14.3 cm. However, increasing the total band $N{\cdot}T$ it will be possible to improve the spatial resolution.

Figs. 6a and 6b show respectively the range profiles of two targets at different absolute distances from the antennas. In all cases, the targets have been detected. Both figures show also that the longer is the distance the harder is to detect the target. In fact, for each range profile, the ratio between the first peak, indicating the target, and the second peak, produced mainly by multiple reflections, decreases with the distance. This is also true for the range profiles with the first subject at 3 and 4 m. In fact, although the first peak at 4 m is slightly higher than the first peak at 3 m, the ratios with their respective second peaks follow the previous consideration. Fig. 7 shows the ratios between the first and the second peaks as function of the absolute distances and considering the targets in frontal

position and at the edge of the antenna beamwidth, namely at about 30 degrees from its line of sight (LoS). These values represent the averages among the results of three measurements for each position. Failures in target localization have occurred at some distances beyond the antenna beamwidth. The target's reflection becomes too weak to be properly detected by the receiver. However, considering that the antenna is placed at the centre of a wall of a 5 x 5 m^2 room, the sideways detection ability of 5 m is deemed unnecessary. Moreover, since a multiple sensor network is planned to be deployed, these angles outside the antenna beamwidth are expected to be covered by the adjacent radar sensors.

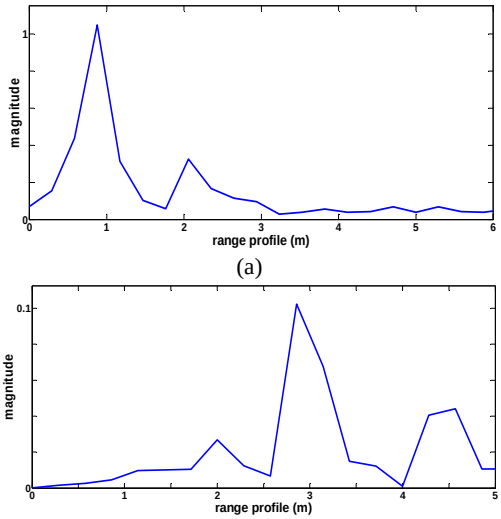

Fig. 5. Measured range profile of a target at 3 m away the antennas before (a) and after (b) compensation and calibration.

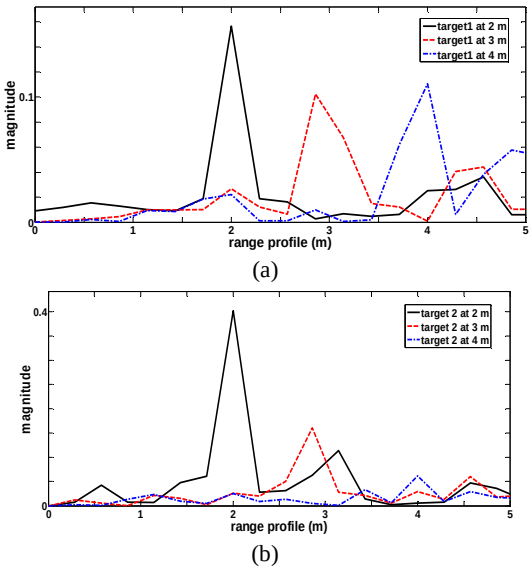

Fig. 6. Measured range profiles of target 1 (a) and target 2 (b) as function of the absolute distances.

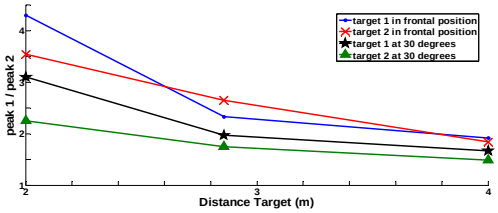

Fig. 7. Ratios between the first and second peaks of target 1 and target 2 as function of the absolute distances and orientations.

V. Conclusion

A technique to make feasible distance measurements of persons in real room environment has been proposed and discussed. Experimental evaluations performed on measurements conducted on real human volunteers have clearly indicated the feasibility of this approach. Moreover, although this approach is demonstrated to be valid for an SFCW radar in this work, the proposed solutions in dealing with practical problems can be also adopted for other ultra-wideband (UWB) radar architectures and applications, such as through-the-wall localization.

Acknowledgement

This work has been supported by FWO-Flanders and KU Leuven GOA project.

References

[1] M. Mercuri, P.J. Soh, L. Boccia, D. Schreurs, G.A.E. Vandenbosch, P. Leroux, and G. Amendola, "Optimized SFCW Radar Sensor Aiming at Fall Detection in a Real Room Environment", *IEEE Topical Conference on Biomedical Wireless Technologies (BioWireless)*, pp. 4-6, Austin, TX, USA, 20-23 Jan. 2013.

[2] F. Ahmad and M. G. Amin, "Noncoherent approach to through-the-wall radar localization," *IEEE Transaction on Aerospace and Electronic Systems*, vol. 42, no. 4, pp. 1405-1419, Oct. 2006.

[3] R. Sorrentino, E. Sbarra, L. Urbani, S. Montori, R.V. Gatti, and L. Marcaccioli, "Accurate FMCW rader-based indoor localization system," *IEEE International Conference on RFID-Technologies and Applications (RFID-TA)*, pp. 362-368, Nice, France, 5-7 Nov. 2012.

[4] K. Yokoo, S. Beauregard, and M. Schneider, "Indoor Relative Localization with Mobile Short-Range Radar," *IEEE Vehicular Technology Conference*, pp. 1-5, Barcellona, Spain, 26-29 April 2009.

[5] C. Zhang, M.J. Kuhn, B.C. Merkl, A.E. Fathy, and M.R. Mahfouz, "Real-Time Noncoherent UWB Positioning Radar With Millimeter Range Accuracy: Theory and Experiment," *IEEE Trans. on Microwave Theory Tech.*, vol. 58, no. 1, pp. 9-20, Jan. 2010.

[6] P. Soh, M. Mercuri, G. Pandey, G.A.E. Vandenbosch, and D. Schreurs, "Dual-band Planar Bowtie Monopole for a Fall-Detection Radar and Telemetry System", *Antennas and Wireless Propagation Letters*, vol. 11, pp. 1698-1701, 2012.